AFRL-RB-WP-TP-2009-3039

PERFORMANCE RESULTS FOR THE OPTICAL TURBULENCE REDUCTION CAVITY (Postprint)

Ryan Schmit, Chris McGaha, John Tekell, Jim Grove, and Michael Stanek

Aerospace Vehicle Integration and Demonstration Branch
Aeronautical Sciences Division

DECEMBER 2008
Interim Report

STINFO COPY

AIR FORCE RESEARCH LABORATORY
AIR VEHICLES DIRECTORATE
WRIGHT-PATTERSON AIR FORCE BASE, OH 45433-7542
AIR FORCE MATERIEL COMMAND
UNITED STATES AIR FORCE

NOTICE AND SIGNATURE PAGE

*//signature//   //signature//

_____   _____
DR. RYAN F. SCHMIT, Aerospace Engineer   MARVIN C. GRIDLEY, Acting Chief
Aerospace Vehicle Integration and   Aerospace Vehicle Integration and
  Demonstration Branch   Demonstration Branch

//signature//

_____
MICHAEL J. STANEK
Technical Advisor
Aeronautical Sciences Division

REPORT DOCUMENTATION PAGE

The public reporting burden for this collection of information is estimated to average 1 hour per response, including the time for reviewing instructions, searching existing data sources, searching existing data sources, gathering and maintaining the data needed, and completing and reviewing the collection of information. Send comments regarding this burden estimate or any other aspect of this collection of information, including suggestions for reducing this burden, to Department of Defense, Washington Headquarters Services, Directorate for Information Operations and Reports (0704-0188), 1215 Jefferson Davis Highway, Suite 1204, Arlington, VA 22202-4302. Respondents should be aware that notwithstanding any other provision of law, no person shall be subject to any penalty for failing to comply with a collection of information if it does not display a currently valid OMB control number. **PLEASE DO NOT RETURN YOUR FORM TO THE ABOVE ADDRESS**.

1. REPORT DATE *(DD-MM-YY)*	2. REPORT TYPE	3. DATES COVERED *(From - To)*
December 2008	Journal Article Postprint	01 December 2006 – 01 December 2008

4. TITLE AND SUBTITLE	5a. CONTRACT NUMBER
PERFORMANCE RESULTS FOR THE OPTICAL TURBULENCE REDUCTION CAVITY (Postprint)	IN-HOUSE
	5b. GRANT NUMBER
	5c. PROGRAM ELEMENT NUMBER
	62201F

6. AUTHOR(S)	5d. PROJECT NUMBER
Ryan Schmit, Chris McGaha, John Tekell, Jim Grove, and Michael Stanek	A0E5
	5e. TASK NUMBER
	5f. WORK UNIT NUMBER
	0A

7. PERFORMING ORGANIZATION NAME(S) AND ADDRESS(ES)	8. PERFORMING ORGANIZATION REPORT NUMBER
Aerospace Vehicle Integration and Demonstration Branch (AFRL/RBAI) Aeronautical Sciences Division Air Force Research Laboratory, Air Vehicles Directorate Wright-Patterson Air Force Base, OH 45433-7542 Air Force Materiel Command, United States Air Force	

9. SPONSORING/MONITORING AGENCY NAME(S) AND ADDRESS(ES)	10. SPONSORING/MONITORING AGENCY ACRONYM(S)
Air Force Research Laboratory Air Vehicles Directorate Wright-Patterson Air Force Base, OH 45433-7542 Air Force Materiel Command United States Air Force	AFRL/RBAI
	11. SPONSORING/MONITORING AGENCY REPORT NUMBER(S)
	AFRL-RB-WP-TP-2009-3039

12. DISTRIBUTION/AVAILABILITY STATEMENT
Approved for public release; distribution unlimited.

13. SUPPLEMENTARY NOTES
PAO Case Numbers: 88ABW-2008-0756; clearance date 31 October 2008. This is a work of the U.S. Government and is not subject to copyright protection in the United States. Document contains color.

14. ABSTRACT
A new optical turbulence reduction cavity model has been built and tested in the Trisonic Gas dynamic Facility (TGF) at Air Force Research Laboratory (AFRL). The new model replaces the 1970's era model and has optical quality fused silica windows that will allow nonintrusive flow field measurements to be made. The results presented in this paper compare the current optical turbulence reduction cavity model with the historic data from the old turbulence reduction cavity model and examines some passive flow control devices.

15. SUBJECT TERMS

16. SECURITY CLASSIFICATION OF:			17. LIMITATION OF ABSTRACT:	18. NUMBER OF PAGES	19a. NAME OF RESPONSIBLE PERSON (Monitor)
a. REPORT	b. ABSTRACT	c. THIS PAGE	SAR	20	Dr. Ryan F. Schmit
Unclassified	Unclassified	Unclassified			19b. TELEPHONE NUMBER *(Include Area Code)* 937-904-8177

Performance Results for the Optical Turbulence Reduction Cavity

Ryan Schmit[*], Chris McGaha[†], John Tekell[‡], Jim Grove[§]

and

Michael Stanek[¶]

Air Force Research Laboratory, Wright-Patterson AFB, OH, 45433, USA

A new optical turbulence reduction cavity model has been built and tested in the Trisonic Gasdynamic Facility (TGF) at Air Force Research Laboratory (AFRL). The new model replaces the 1970's era model and has optical quality fused silica windows that will allow non-intrusive flow field measurements to be made. The results presented in this paper compare the current optical turbulence reduction cavity model with the historic data from the old turbulence reduction cavity model and examines some passive flow control devices.

I. Introduction

In the mid 1970's, the Turbulence Reduction cavity model was built and tested in the Trisonic Gasdynamic Facility at Wright-Patterson Air Force Base. This model was used numerous times over a period of about 15 years and provided insight into controlling acoustic noise generated by a rectangular cavity with an L/D of 5.6.

Since then numerous wind tunnel tests have examined flow control techniques to reduced Rossiter tone and overall sound pressure levels inside the cavity. The one issue that has been hard to determine is the physical effect these actuators have on the flowfield. With current off-body flow diagnostic techniques like Particle Image Velocimetry (PIV) and Laser Doppler Anemometry (LDA), the one requirement that is needed for these methods is to have optical access for viewing the particulate as it tracks with the flowfield. Though only a few university facilities have successfully seeded a cavity and obtained PIV and/or LDA measurements of the baseline flow (Murray,[1] Murray[2]), fewer have obtained measurements with modern flow control techniques.

In this paper we are examining different flow control devices that significantly reduce the frequency spectrum, Rossiter tones and the Overall Sound Pressure Levels (OASPL) so that in the near future we can examine and study their effects on the flow fields surrounding the cavity by using non-intrusive diagnostic techniques.

II. Experimental Setup

A. Optical Turbulence Reduction Cavity Model

The Turbulence Reduction Cavity model tested from the mid 1970's to the late 1980's did not provide the optical access necessary for current state of the art non-intrusive flow field measuring techniques. Therefore, a new Optical Turbulence Reduction Cavity model with optical windows was built for the TGF. Figure 1 shows the new optical cavity model inside the Trisonic Gasdynamic Facility. The cavity dimensions are: length 8.5 inches, depth 1.5 inches and width 2.5 inches, the L/D is 5.67 and the model scale is approximately

---

[*]Aerospace Engineer, AFRL/RBAI, 2130 8th Street, and AIAA Member
[†]Aerospace Engineer, AFRL/RBAI, 2130 8th Street
[‡]Test Engineer, AFRL/RBAI, 2130 8th Street
[§]Weapons Integration Team Lead, AFRL/RBAI, 2130 8th Street
[¶]Technical Advisor, AFRL/RBAI, 2130 8th Street

American Institute of Aeronautics and Astronautics

$1/20^{th}$. The fore body of the model is 7.0 inches long and is $5in$ wide. The cavity model can be pitched from $0°$ to $-3.0°$ to form an attached boundary layer along the leading edge of the cavity.

There are three interchangeable optical quality fuse silica windows for this model, the two side wall, as shown in Figure 1, and the ceiling. The ceiling window is interchangeable with an aluminum blank that contains temperature, static and dynamic pressure sensors. There are 15 dynamic pressure sensor located throughout the cavity. Four of these sensors are in the forward actuator block, 4 in the aft block and 7 in the ceiling of the cavity, locations shown in Table 1. Two thermal couples and 5 static pressure ports are also included in the ceiling. One feature of the current model is the ability roll the cavity from $0°$ to $30°$, $45°$ and $90°$ so that cavity can be positioned for proper alignment with current non-intrusive flow diagnostic techniques.

Table 1. Sensor positions on ceiling of cavity

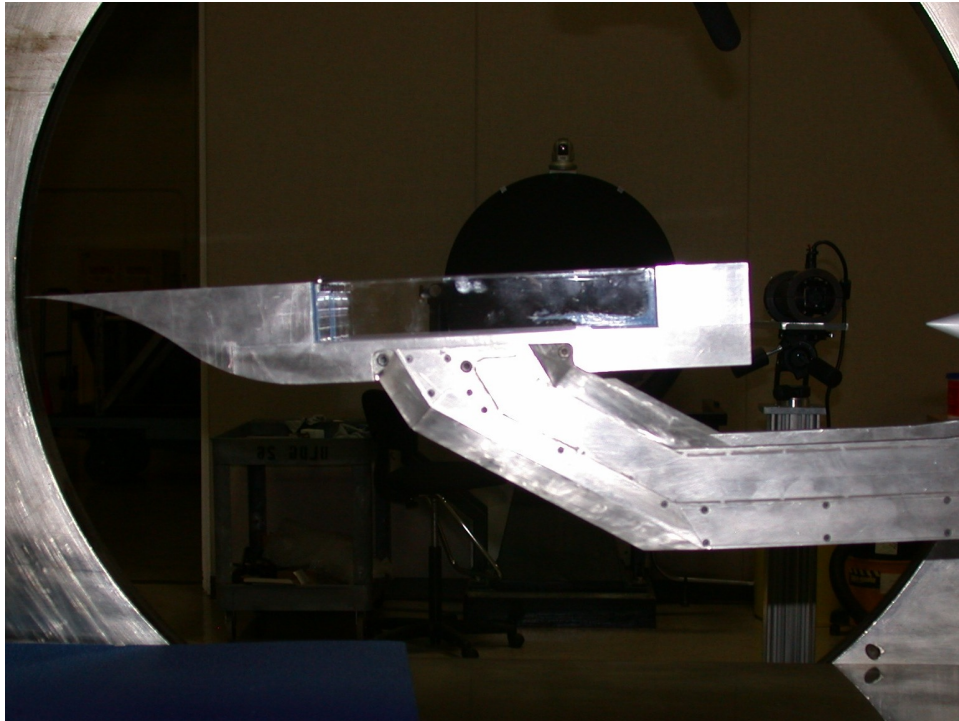| Sensor	x/l	$2y/w$
1	0.073	0.000
2	0.229	0.000
3	0.379	0.000
4	0.529	0.120
5	0.679	0.000
6	0.829	0.000
7	0.979	0.000

Figure 1. The Optical Turbulence Reduction Cavity Model mounted inside the Trisonic Gas

B.   Flow Control Devices

Four flow control devices were tested and they are: the sawtooth spoiler, the flat spoiler, the $3mm$ rod and the $6mm$ rod in the cross flow.

American Institute of Aeronautics and Astronautics

Many studies including Heller and Bliss,[3] Kaufman and Clark,[4] Shaw et al.,[5] Sarno and Franke[6] have examined zero-frequency devices like spoilers to suppress the sound pressure levels inside the cavity. All the previous studies have concluded that spoilers at the leading edge of a cavity provided the greatest sound pressure level suppression because they lift the upstream boundary layer. The shear layer instability that grows from the lifted boundary layer flow will have a reduced impingement effect on the rear wall of the cavity, thereby reducing the sound pressure levels. These suppression devices are dependent on the frequency mode of the cavity and the upstream Mach number.[7]

The sawtooth and flat spoilers are shown in Figure 2. Both spoilers spanned the cavity and are 2.5 inch wide, they protrude 0.160 inches above the cavity waterline and they are 0.063 inches thick. The sawtooth spoiler has ten teeth with a 0.25 inch spacing and the valley depth of 0.120 inches.
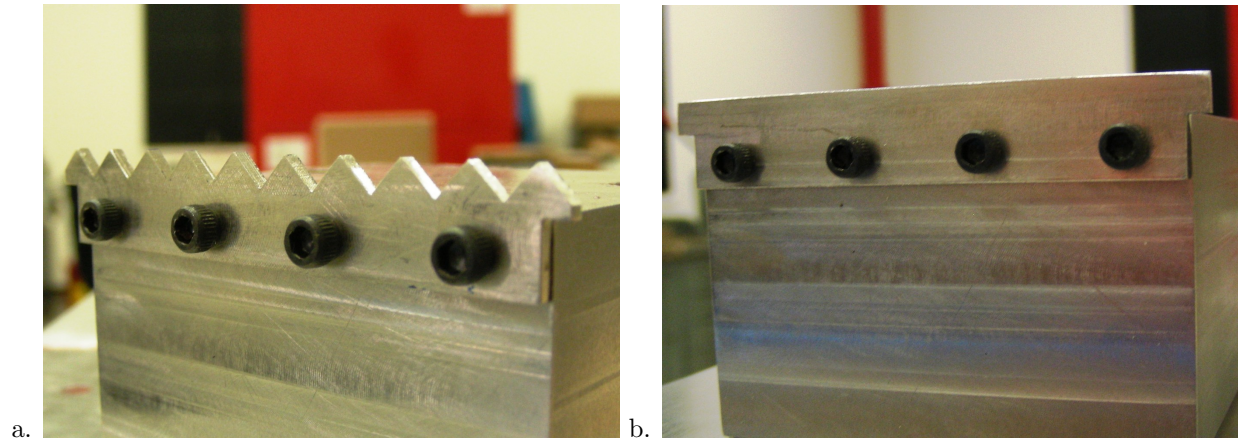

a.

b.

Figure 2. a.) Sawtooth and b.) Flat Spoilers used for historic data comparison.

Stanek[8] describes the development and theory behind the rod in a crossflow as it pertains to a high frequency flow control device. The rod's basic theory is that the shedding produced by the rod breaks up the coherence downstream resulting in suppression. The basic parameters for the rod are: the rod diameter is only 2/3 the boundary layer thickness, the gap distance should be 2/3 the boundary layer thickness so that the rod has subsonic flow to produce the shedding.

The two rods in a cross flow are shown in Figure 3. The rods are ceramic $3mm$ and $6mm$ in diameter and are 2.5 inch wide. They are held in position using two vertical posts that are $8mm$ in diameter. These posts adjust the gap between the cavity waterline and the rod itself.
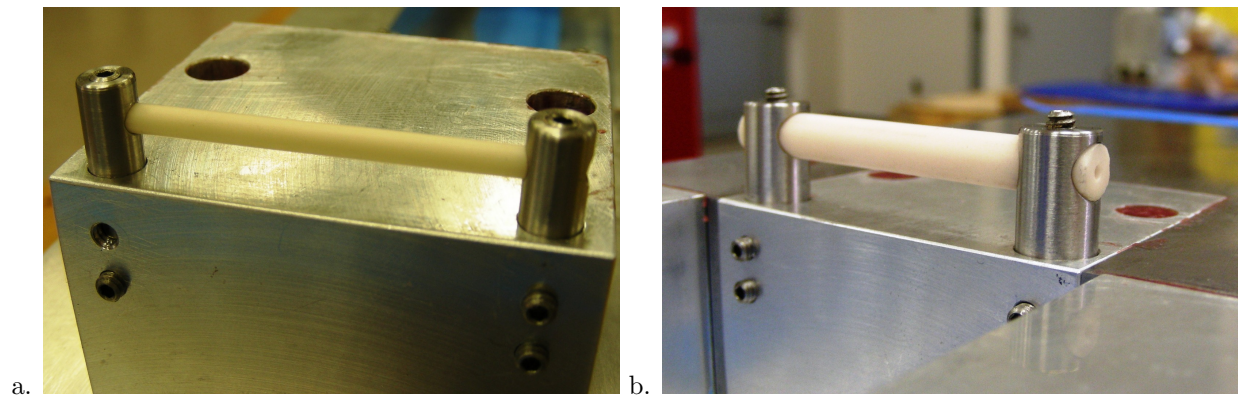

a.

b.

Figure 3. a.) $3mm$ Rod and b.) $6mm$ Rod

American Institute of Aeronautics and Astronautics

C.   Trisonic Gasdynamic Facility (TGF)

The Trisonic Gasdynamic Facility shown in Figure 4, located in building 26 in Area B of WPAFB, was built in the 1950's to provide research of complex flow configuration vehicles in the sub and supersonic regime to researchers within the Air Force and DoD organizations. When coupled, the 1500 hp and 3500 hp motors provides the power to this closed circuit wind tunnel to achieve a test velocity of Mach 0.23 to 0.87, and 1.5, 1.9, 2.3 and 3.0 by changing nozzle blocks, with pressures ranging from 0.5 to 2.0 atmospheres. The maximum subsonic Reynolds number for the tunnel is $2.5x10^6$ and the maximum subsonic dynamic pressure is 350 psf.[9] The maximum supersonic Reynolds number is $5x10^6$ and the maximum supersonic dynamic pressure is 1000 psf.[9] The stagnation temperature is held constant at $85°$ F.

Figure 4. Trisonic Gasdynamic Facility

The test section is two feet high, two feet wide, four feet long with two flat viewing windows on either side that are 30.34 inches diameter. The primary model support, a crescent mounted sting, which can be used to reach various attitudes, or model orientations, including pitching from $-1°$ to $+18.5°$, roll $-90°$ to $+180°$, and has the capability to do half-span testing. Refer to the TGF User's Manual[10] for more information and capabilities.

D.   Data Acquisition and Reduction

A high speed data acquisition system was built to support this test. The dynamic pressure sensors were sampled at $85kHz$ and low passed filtered at $42.5kHz$. To verify the new high speed data acquisition system was working as expected, the data acquired was compared to Kaufman and Clark[4] at similar running conditions.

Figure 5 shows the spectrum pressure level and overall sound pressure level data at the aft wall of the cavity when the turbulence reduction cavity was tested in the early 1980's. This data was taken at Mach 0.74 for an L/D of 5.6 cavity at an angle of attack of $-3/4°$. The dashed lines are the theoretically predicted Rossiter tones.[4]

Figure 6 shows the current cavity baseline and sawtooth spoiler spectrum and overall sound pressure levels. The current test conditions are Mach 0.75, Reynolds number of $2x10^6$ with a pitch angle of $-3.0°$. The result compare well with the Kaufman's data, Figure 5. The 1st, 2nd and 3rd Rossiter tones are nearly the same frequency and loudness.

There are some slight differences between the two tests: Mach number, Pitch Angle, and Reynolds Number. The Mach number difference is 0.01 and the Pitch Angle difference is $2.75°$. The Reynolds number difference is between $6x10^4$ and $4x10^5$ because specific Reynolds number was not mentioned in the Kaufman report.

A significant difference between the two tests is the processing of the data. The details for the processing routine for Kaufman data are unknown. But the current data was collected such that 102400 simultaneous samples were taken on all available dynamic pressure transducers. Each signal was broken into twenty five
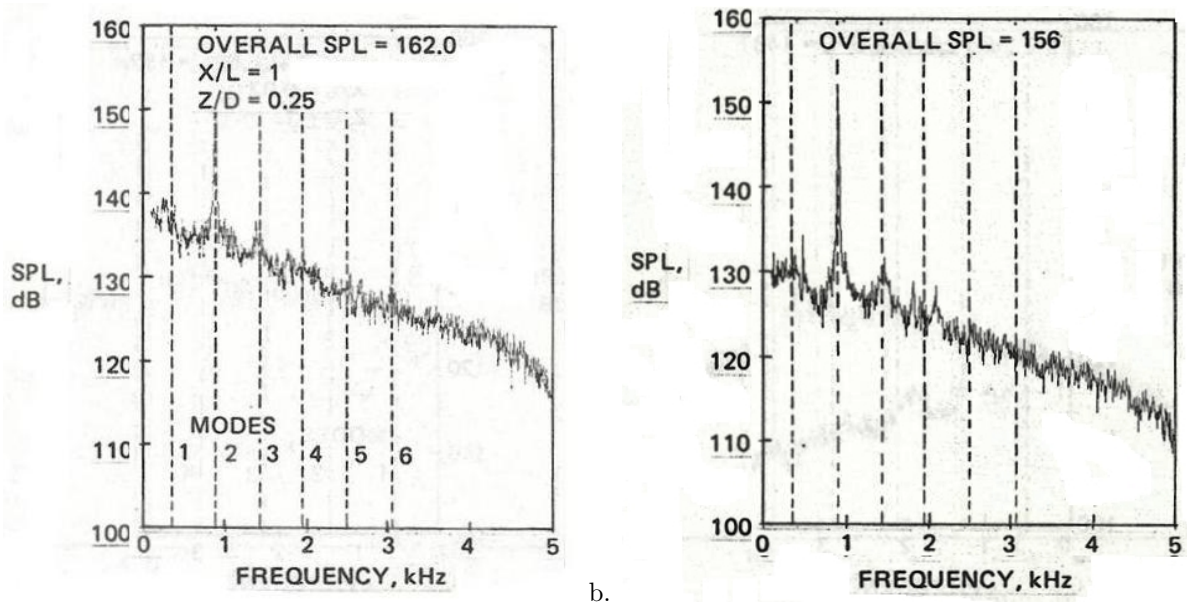
a.   b.

Figure 5. Kaufman and Clark[4] a.) Baseline and b.) Sawtooth Spectrum Pressure Levels on Aft Wall of the Cavity, Mach .74, $\alpha = -3/4°$

4096 sample blocks. A Hanning window was applied to each data block then the spectrum was determined. An ensemble average of the spectrum was determined and is shown as the results. The OASPL was integrated from $100Hz$ to $20kHz$.
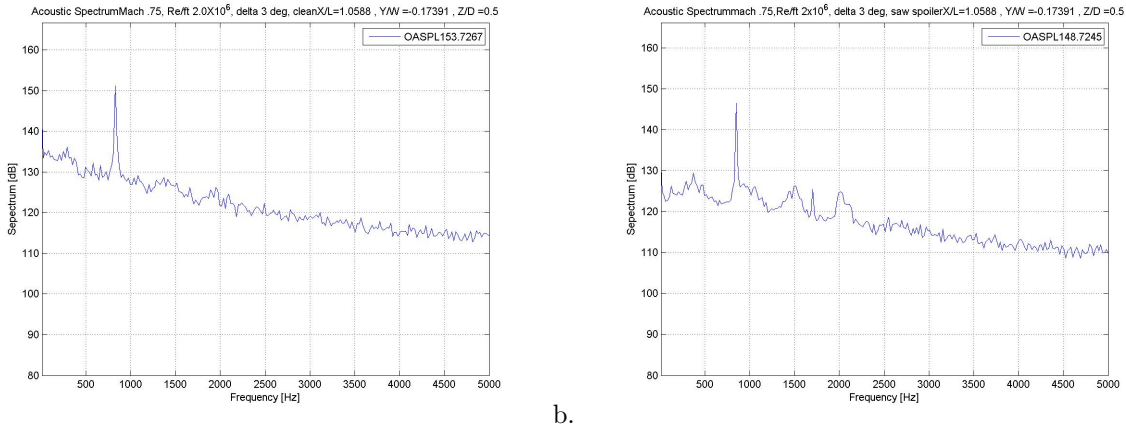

a.   b.

Figure 6. a.) Baseline and b.) Sawtooth Spectrum Pressure Levels on Aft Wall of the Cavity, Mach .75, $\alpha = -3.0°$

III.   Results

A.   Boundary Layer

Figure 7 shows the boundary layer rake used in the current test. Not all tubes were utilized do to the limited internal passageways inside the model. Table 2 shows the tube's position and the corresponding height from the wall.

Figure 8a shows boundary layer data from Clark[11] at Mach 0.7 for Reynolds numbers of $3x10^6$ and $5x10^6$ with and without a trip at a pitch angle of $-.75°$. Figure 8b shows the current measurement of the boundary
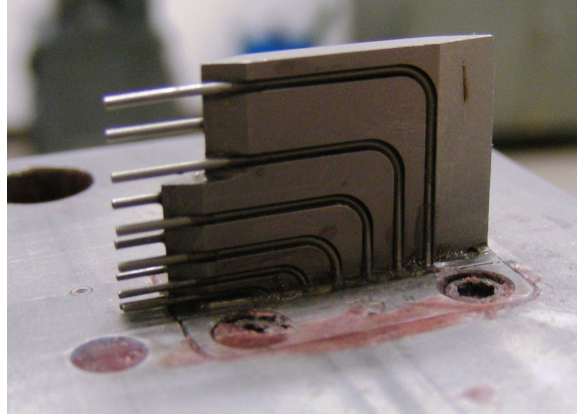
American Institute of Aeronautics and Astronautics

Figure 7. Boundary Layer Rake

Table 2. Boundary Layer Tube Position and Height

1	0.009 in
3	0.075 in
4	0.110 in
5	0.150 in
6	0.190 in
7	0.235 in
8	0.450 in

American Institute of Aeronautics and Astronautics

layer at Mach 0.7 Reynolds number of $2x10^6$ without a trip at a pitch angle of $-.75°$.

Both measurements indicate a thicker layer than theory dictates. Using law of the wall theory the boundary layer thickness should be on the order of 0.236 inches. Examining the current measurements shows a substantiality thicker boundary layer than even the Clark data. Further examination of this boundary layer is needed in future tests to properly resolve this issue.
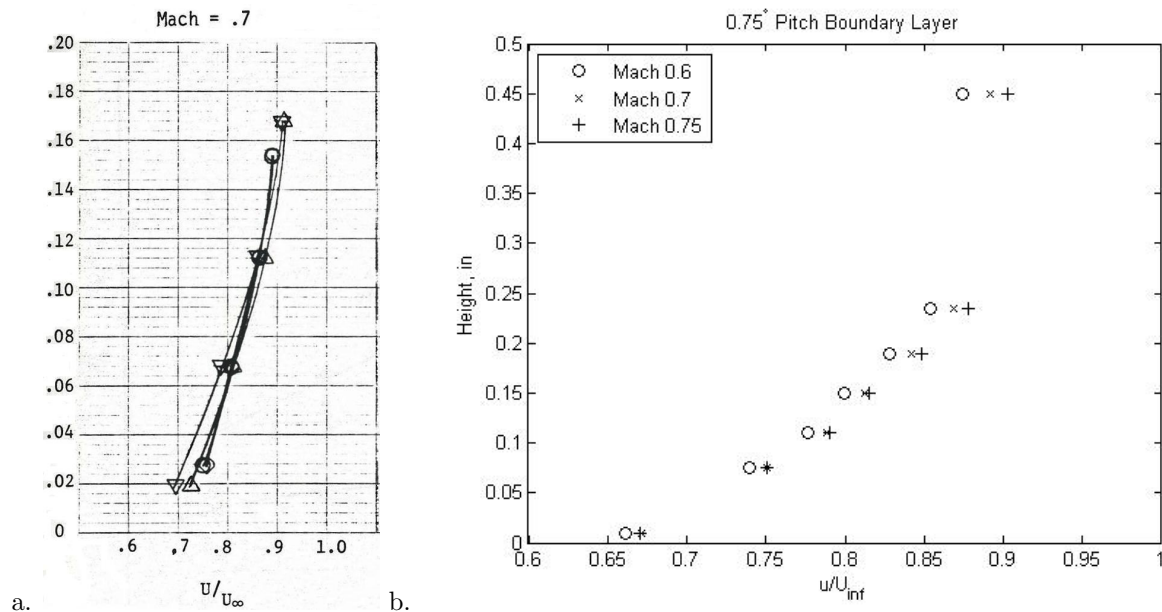

Figure 8. a.) Mach 0.7 Boundary Layer Data from Clark.[11] b.) Boundary Layer Thickness vs. Pitch Angle at Varying Mach with a Re # $2*10^6$

B. Spectrum Results

Figure 9a shows the baseline's, clean cavity, spectrum pressure levels on the aft wall of the cavity at varying Mach numbers at an angle of attack of $-3.0°$. As expected Mach 0.3 and 0.4 has no Rossiter tones. As the Mach number increases the second and third tones become very prevalent with the max peak at $152dB$ at Mach 0.75. The Mach 1.5 case has five distinct Rossiter tones.

Figure 9b shows the baseline's, clean cavity, overall sound pressure levels throughout the cavity for the different Mach numbers at a Reynolds number of $2x10^6$ at a pitch angle of $-3.0°$. As in past experiments the aft wall of the cavity is the loudest with the Mach 0.75 and 1.5 being the worst cases possible with OASPL of $153dB$ and $152dB$ respectively.

Figure 10a shows the comparison of four flow control devices used at suppressing the acoustic signature on the aft wall of the cavity. The $3mm$ and $6mm$ rods were $2mm$ and $2.66mm$ respectively above the waterline for this part of the test. All four flow control devices show suppressing effects on the acoustic signature with the $6mm$ rod working the best by significantly reducing the Rossiter tone. The spoilers and the $3mm$ rod only reduce the Rossiter tone by a few decibels but they do reduce the OASPL by nearly $5dB$ to $10dB$ as shown in Figure 10b. Figure 10b shows the OASPL throughout the cavity and the effects of the flow control device has on the OASPL. As noted earlier the $6mm$ rod reduces the OASPL on the aft wall by $15db$, which is a significant amount, as well as the rest of the cavity.

C. Varying the Rod's Gap

When examining Figure 10 it can be noted that the two rods do not appear to be shedding as mention above by Stanek.[8] One reason that the shedding does not appear in Figure 10 is the fact that this data was taken on the aft wall of the cavity. This was also noted by Stanek because the coherence of the shedding would break down prior to its arrival to the aft wall and therefore no sensor would see the shedding. By examining data upstream of the aft wall, especially the closer sensors to the rod the shedding frequency could
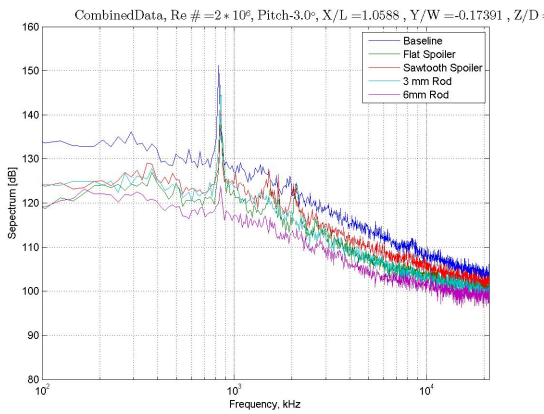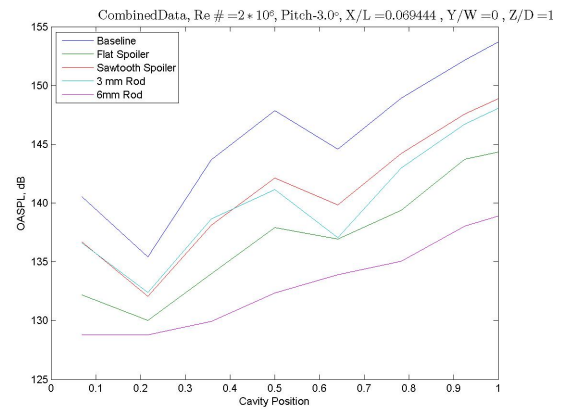
American Institute of Aeronautics and Astronautics
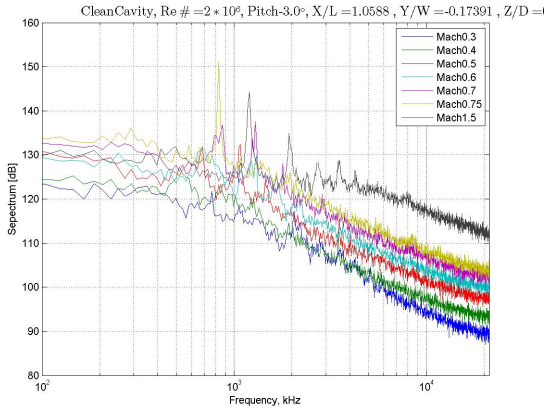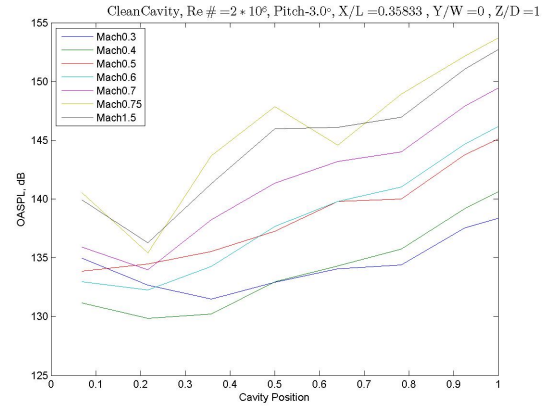
Figure 9. a.) Baseline Frequency Spectrum with vary Mach number at Re # $2x10^6$ at Pitch Angle of $-3.0°$ b.) Baseline Overall Sound Pressure Level throughout the bay with vary Mach number at Re # $2x10^6$ at Pitch Angle of $-3.0°$

Figure 10. a.) Frequency Spectrum of 4 Different Flow Control Methods at Mach 0.75, Re # $2x10^6$, Pitch angle of $-3.0°$ compared with the Baseline Spectrum. b.) OASPL throughout the cavity with 4 Different Flow Control Methods at Mach 0.75, Re # $2x10^6$, Pitch angle of $-3.0°$ compared with the Baseline Spectrum

American Institute of Aeronautics and Astronautics

be captured. After examining the companion data to Figure 10 it was observed that the rods shedding was not clearly observable. Because the rod is dependent on the boundary layer thickness for location and sizing and the fact that boundary layer measurements were inconclusive the two rods' gap heights were varied to determine the optimal position.

Figure 11a and b shows the frequency spectrum of the $3mm$ rod as the gap between the rod and the waterline was varied at Mach 0.75, Reynolds Number $2x10^6$. Figure 11c and d show the OASPL throughout the cavity as the $3mm$ rod gap height was varied. Note that the pitch angle for these results are at $-0.75°$. Examining the frequency spectrum the $3mm$ rod sheds around 13 kHz when the gap is greater than 0.25 inches. When the gap is below the 0.25 inches the rod stops shedding because the gap is too narrow for the shedding event to occur. The interesting part is the OASPL is reduced the most by 15 dB at the aft wall when the $3mm$ rod has a gap of 0.101 and 0.190 inches as shown in Figure 11c. When the rod gap is greater the OASPL is reduced approximately 11 dB even though shedding is occurring. These two $3mm$ rod condition will need to be examined further with non-intrusive flow diagnostic techniques to further understand the nuances.
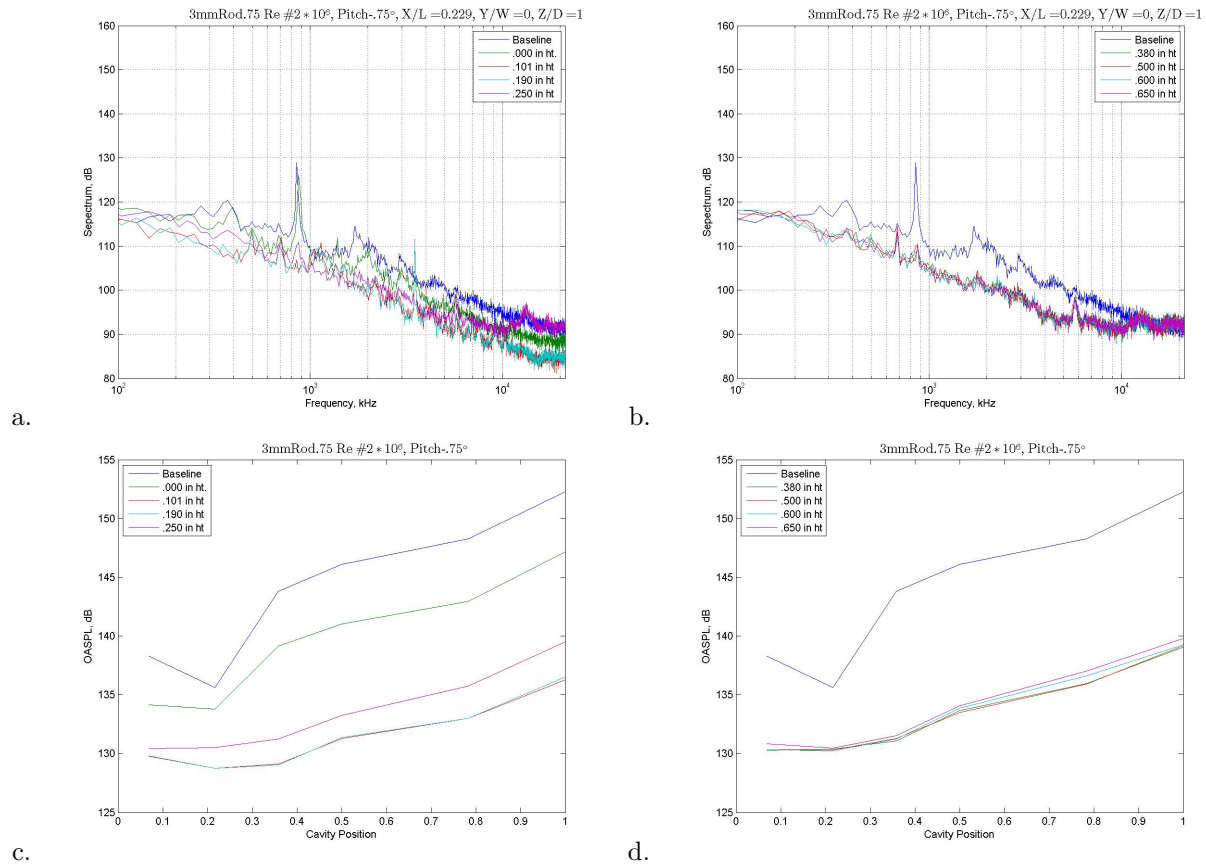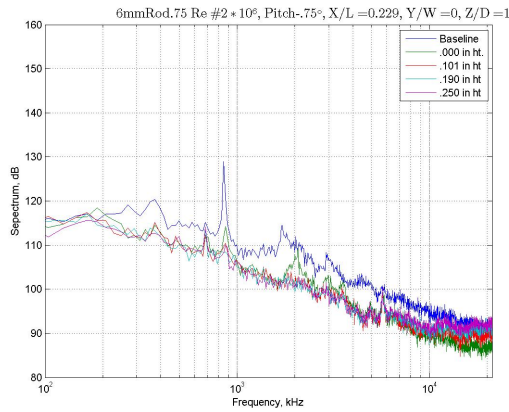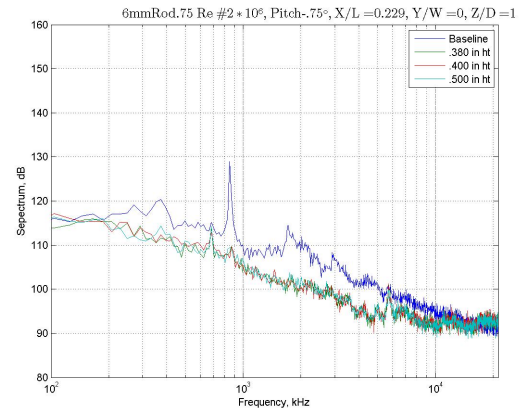

a.

b.

c.

d.

Figure 11. a.) and b.) Frequency spectrum of the $3mm$ rod with varying gap heights at Mach 0.75, Re # $2x10^6$, Pitch angle of $-0.75°$ and compared with the baseline frequency spectrum. c.) and d.) OASPL throughout the cavity of the $3mm$ rod with varying gap heights at Mach 0.75, Re # $2x10^6$, Pitch angle of $-0.75°$ and compared with the Baseline Spectrum
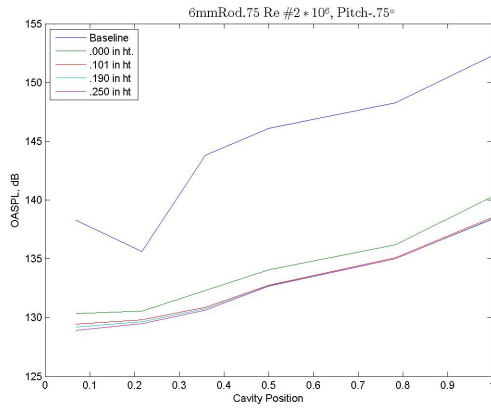
Figure 12a and b shows the frequency spectrum of the $6mm$ rod as the gap between the rod and the waterline was varied. Figure 12c and d show the OASPL throughout the cavity as the $6mm$ rod gap height was varied. Note that the pitch angle for these results are at $-0.75°$. Examining the frequency spectrum the $6mm$ rod sheds around 12 kHz when the gap was present. By comparing Figure 11c and d to Figure 12c and d it can be seen that the $3mm$ rod out performs the $6mm$ rod. Again no definitive explanation as to why this occurs can be concluded at this time.

American Institute of Aeronautics and Astronautics

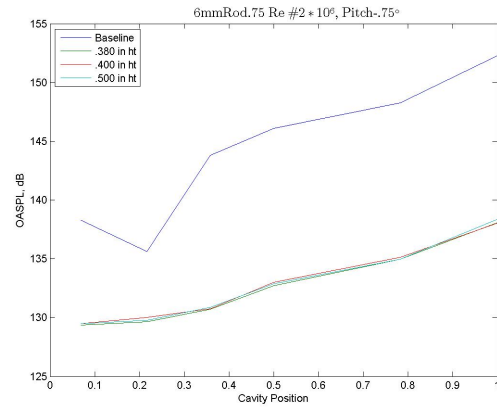**Figure 12. a.) and b.) Frequency spectrum of the 6mm rod with varying gap heights at Mach 0.75, Re # $2x10^6$, Pitch angle of $-0.75°$ and compared with the baseline frequency spectrum. c.) and d.) OASPL throughout the cavity of the 6mm rod with varying gap heights at Mach 0.75, Re # $2x10^6$, Pitch angle of $-0.75°$ and compared with the Baseline Spectrum**

D.   Cross Correlation and Wavenumber

Figure 13 shows the cross correlation for the baseline and three different flow control configurations at Mach 0.75. Four dynamic pressure sensors located throughout the cavity and the aft wall were used to create the correlations. Figure 13a shows the baseline with Rossiter tone produced a clean correlation which shows the forward half of the cavity is out of phase with the aft half. Figure 13b show the cross correlation decays using the $3mm$ rod with a gap of 0.19 inches. Figure 13c show the cross correlation decays using the $3mm$ rod with a gap of 0.25 inches. Figure 13d show the cross correlation decays using the $6mm$ rod with a gap of 0.25 inches.

Using the cross correlation can determine the convective speed of the shear layer flow, for a cavity the main initiator of the convective velocity is the Rossiter tone. Therefore, when the Rossiter tone is suppressed as in Figures 13b, c, and d, the convective velocity increases because the scales of the shear layer are smaller. The nuances between the cross correlation for each of the three suppressed cases are unknown at this time until the shear layer can be further examined using non-intrusive diagnostic technique.
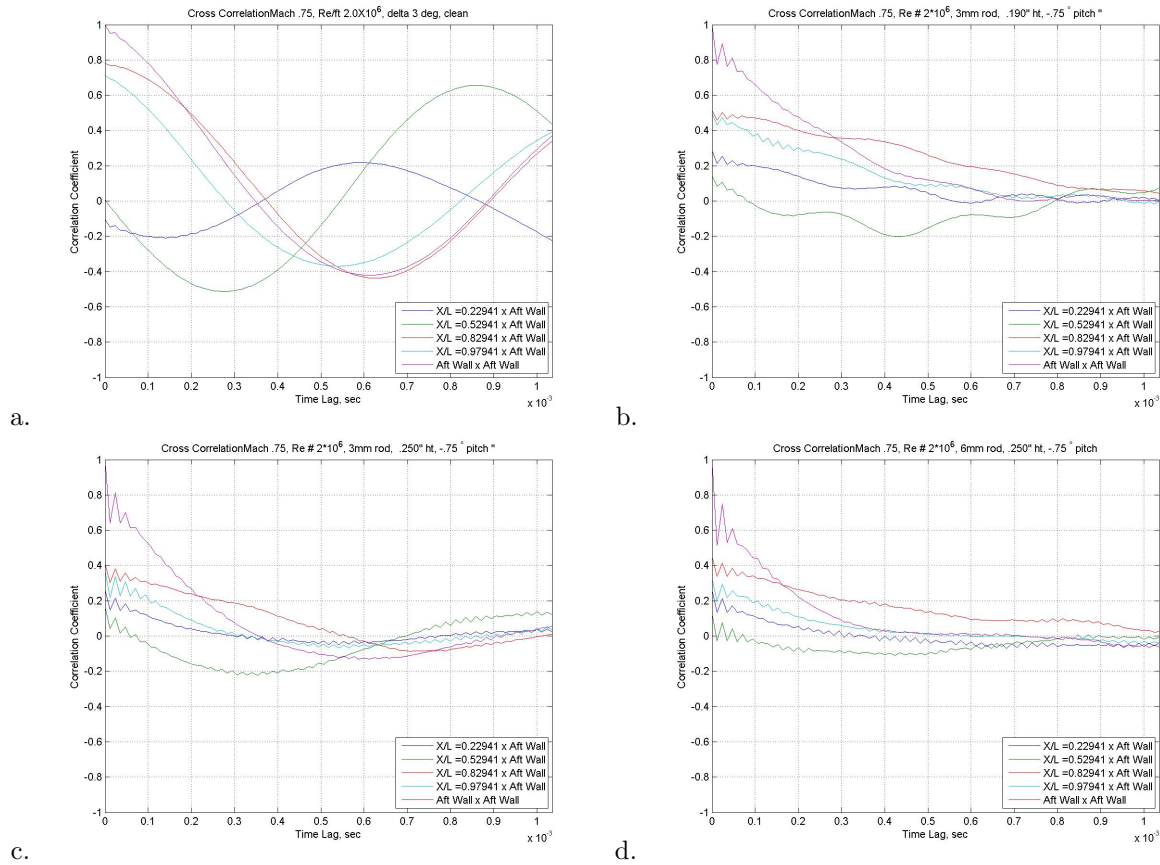

a.   b.   c.   d.

Figure 13.   a.)   Cross Correlation of the baseline cavity at Mach 0.75 and −3.0° pitch angle.   b.)   Cross Correlation using the 3mm rod with a .190 inch gap Mach 0.75 and −.75° pitch angle.   c.)   Cross Correlation using the 3mm rod with a .250 inch gap Mach 0.75 and −.75° pitch angle.   d.)   Cross Correlation using the 6mm rod with a .250 inch gap Mach 0.75 and −.75° pitch angle.

Bassioni et al.[12] examined a cavity with an aspect ratio L/D of 5 at a low speed Mach of 0.086. They were able to separate the acoustic and hydrodynamic pressure waves that travel through the cavity using wavenumber-frequency spectrum analysis. Other research has also used this analysis like Hudy et al.[13] and Zhang and Naguib[14] on cavity and backward facing steps.

Figure 14 shows the wavenumber-frequency spectrum for the baseline and three different flow control configurations at Mach 0.75. In the figures, the magnitude of the spectrum is displayed using a color scale. It should be noted that the results have been normalized by the largest spectrum magnitude. Figure 14a shows the baseline wavenumber-frequency spectrum with the Rossiter tone clearly seen at a shedding fre-

quency of 0.75 and a wave mode of ±1 and ±3. Figure 14b show the $3mm$ rod with a gap of 0.19 inches wavenumber-frequency spectrum. Figure 14c show the $3mm$ rod with a gap of 0.25 inches wavenumber-frequency spectrum. Figure 14d show the $6mm$ rod with a gap of 0.25 inches wavenumber-frequency spectrum.

Since the slope is positive in the right-half plane and negative in the left-half plane, peaks found in the right-half plane are associated with downstream-traveling disturbance and peaks in the left-half plane are associated with upstream-traveling disturbance.[12] Examining the differences the controlled cases distribute the disturbances over the entire frequency range instead of it being concentrated one or two Rossiter tones. Again the nuances between the wavenumber-frequency spectrum for each of the three suppressed cases are unknown at this time until the shear layer can be further examined using non-intrusive diagnostic technique.
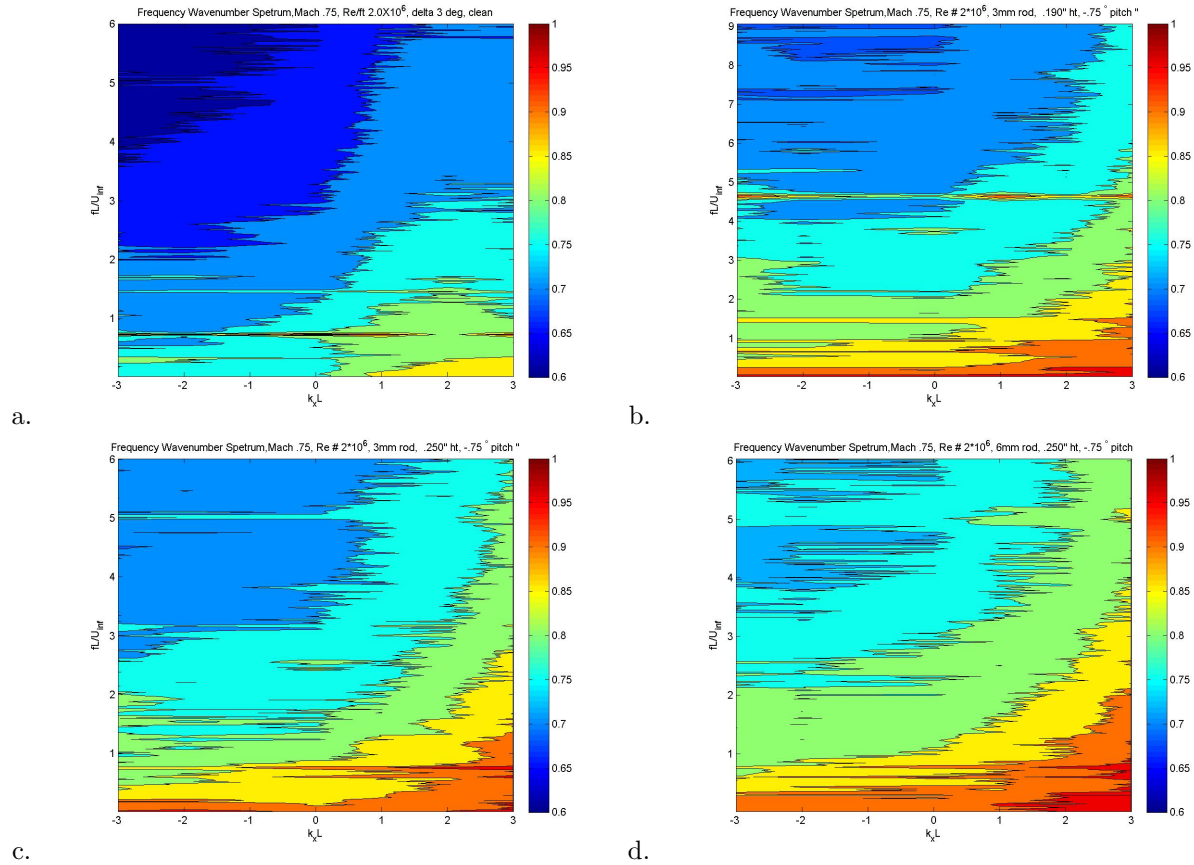

Figure 14. a.) Wavenumber vs Frequency Spectrum of the baseline at Mach 0.75 and $-3.0°$ pitch angle. b.) Wavenumber vs Frequency Spectrum using the $3mm$ rod with a .190 inch gap Mach 0.75 and $-.75°$ pitch angle. c.) Wavenumber vs Frequency Spectrum using the $3mm$ rod with a .250 inch gap Mach 0.75 and $-.75°$ pitch angle. d.) Wavenumber vs Frequency Spectrum using the $6mm$ rod with a .250 inch gap Mach 0.75 and $-.75°$ pitch angle.

IV.   Conclusion

The testing of a new optical turbulence reduction cavity model for the Trisonic Gasdynamic Facility (TGF) has occurred. The current model was compared with an older model that produced very similar frequency spectrum and OASPL. The boundary layer thickness is still unknown at this time and will be investigated in future tests.

Overall, the test has indicated that there are several flow control candidates that can suppress the Rossiter tone and reduce the overall sound pressure level quite well. These candidates will be examined closer when non-intrusive diagnostic techniques are used to measure the flow field surrounding the cavity in future tests.

American Institute of Aeronautics and Astronautics

References

[1]Murray, N. E. and Ukeiley, L. S., "Flow Field Dynamics in Open Cavity Flows," *AIAA Paper 2006-2428*, 12th AIAA/CEAS Aeroacoustics Conference (27th AIAA Aeroacoustics Conference), May 2006, p. 16.

[2]Murray, N. E., Ukeiley, L. S., and Raspet, R., "Calculating Surface Pressure Fluctuations from PIV Data Using Poisson's Equation," *AIAA 2007-1306*, 45th AIAA Aerospace Sciences Meeting and Exhibit, Jan 2007, p. 15.

[3]Heller, H. H. and Bliss, D. B., "The physical mechanism of flow-induced pressure fluctuations in cavities and concepts for their suppression," *AIAA 1975-491*, 2nd AIAA Aero-Acoustics Conference, 1975, see also report AFFDL-TR-74-133, p. 9.

[4]Kaufman, L. G. and Clark, R., "Mach 0.6 to 3.0 Flows Over Rectangular Cavities," AFWAL-TR-82-3112, Air Force Research Laboratory, May 1983.

[5]Shaw, L. L., Bartel, H., and McAvoy, J., "Prediction and Suppression of the Acoustic Environment in Large Enclosures With a Small Opening Exposed to Aerodynamic Flow," *AIAA 1982-0121*, ASIA 20th Aerospace Science Meeting, 1982, p. 9.

[6]Sarno, R. L. and Franke, M. E., "Suppression of Flow-Induced Pressure Oscillations in Cavities," *Journal of Aircraft*, Vol. 31, No. 1, Jan - Feb 1994, pp. 90–96.

[7]Schmit, R. F. and Raman, G., "High and low Frequency actuation comparison for a weapons bay cavity," *International Journal of Aeroacoustics*, Vol. 5, No. 4, 2006.

[8]Stanek, M. J., *A Numerical Study of the Effect of Frequency of Pulsed Flow control Applied To A Rectangular Cavity in Supersonic Crossflow*, Ph.D. thesis, Univeristy of Cincinnati, Ohio, July 2005.

[9]Guyton, R. W., "Test Summary: Parametric Nozzle - Phase III - TGF Test 256," AFWAL-TM-86-176-FIMM, Air Force Research Laboratory, Dec 1985.

[10]Clark, G. F., "Tri-soncic Gas-dynamic Facility User's Manual," AFWAL-TM-82-176-FIMM, Air Force Research Laboratory, Apr 1982.

[11]Clark, R. L., "Weapons Bay Turbulence Recution Techiques," AFFDL-TM-75-147-FXM, Air Force Research Laboratory, Dec 1975.

[12]Bassioni, I., Abdelkhalek, M., Ghoneim, Z., Daoud, M., and Naguib, A. M., "Mircrophone-Array Measurements of Acoustic and Hydrodynamic Wall-Pressure Fluctuations in a Low-Speed CAvity Flow," *AIAA 2004-2655*, 34th AIAA Fluid Dynamics Conference and Exhibit, 2004, p. 9.

[13]Hudy, L. M., Naguib, A. M., and Jr., W. M. H., "Wall-pressure-array measurments beneath a separating/reattaching flow region," *Physics of Fluids*, Vol. 15, No. 3, 2003.

[14]Zhang, K. and Naguib, A. M., "Effect of Cavity Width on the Unsteady Pressure in a Low-Mach-Number Cavity," *AIAA Journal*, Vol. 46, No. 7, 2008.